Physica C 470 (2010) 914–917

Contents lists available at ScienceDirect

Physica C

journal homepage: www.elsevier.com/locate/physc

Understanding the role of heavy ion-irradiation induced surface columnar nanostructures through FESEM imaging

Angelica Chiodoni [a,b], Francesco Laviano [a,c], Roberto Gerbaldo [a,c], Gianluca Ghigo [a,c], Laura Gozzelino [a,c], Enrica Mezzetti [a,c], Bruno Minetti [a,c,*], Wai K. Kwok [d]

[a] Dept. of Physics, Politecnico di Torino, C.so Duca degli Abruzzi 24, Torino 10129, Italy
[b] Materials and Microsystems Laboratory (χLAB), Politecnico di Torino, C.so Duca degli Abruzzi 24, Torino 10129, Italy
[c] Istituto Nazionale di Fisica Nucleare (INFN), Sezione di Torino, V.P. Giuria 1, Torino 10125, Italy
[d] Materials Science Division, Argonne National Laboratory, 9700 South Cass Avenue, Argonne, IL 60439, USA

ARTICLE INFO

Article history:
Available online 20 February 2010

Keywords:
High-temperature superconductors
Columnar nanostructures
Blind holes
FESEM imaging

ABSTRACT

In this paper we report on the effects of "surface columnar defects" (blind holes) generated by heavy ion irradiation by performing Field Emission Scanning Electron Microscopy (FESEM) imaging of the columns created across a selected set of specimens, ranging from $YBa_2Cu_3O_{7-x}$ melt-textured bulks and $Bi_2Sr_2Ca_2Cu_3O_x$ monofilamentary tapes to $YBa_2Cu_3O_{7-x}$ single crystals. Different ion fluences, resulting into modifying the superconducting properties, were sampled. A correlation between FESEM patterns and volume integrated measurements shows how surface columnar defects claim the leadership of the superconducting behaviors of the ion implanted samples.

1. Introduction

Heavy ions crossing high temperature superconducting (HTS) materials [1] – either bulk materials, multilayer film structures over any substrate, or single crystals – have the power to implant across such systems nanometric sized 3D amorphous columnar structures [2].

Columns with moderate density were widely exploited as excellent flux pinning centers for superconducting vortices, working especially at higher temperatures where new phases, not attainable with other kinds of defects, were exhibited (e.g. Bose-Glass phase [3]). For large enough ion fluences the material can be modified in such a way that it starts exhibiting its own critical temperature (T_c) [4].

The focus of the present paper is indeed to emphasize through direct structural imaging how the power of truncated columns (blind holes) is so high to be in charge of strongly modified superconducting properties of the samples also when only a fraction of the volume is involved [5–7].

We implanted gold ions of 0.25 GeV into a set of specimens ranging from $YBa_2Cu_3O_{7-x}$ (YBCO) melt-textured bulks and $Bi_2Sr_2Ca_2Cu_3O_x$ (Bi-2223) monofilamentary tapes to YBCO single crystals. The irradiations were performed at INFN Labs by employing Tandem accelerators.

The insight offered by FESEM imaging (ZEISS Supra 40 Field Emission Scanning Electron Microscopy) is crucial to outline that the effect of truncated ion-induced columns or "blind holes" [7,8] can be enhanced by the other defects playing an ancillary role.

In this paper we show how the FESEM imaging allows one to visualize such kind of truncated columns as well as ancillary defects, and to evaluate column distribution, size and implantation depth [7]. Several specimens of different preparations were cleaved along the irradiation direction to visualize and to optimize the imaging. Volume susceptometric and magnetometric measurements are put in tight correlation with images.

2. Results and discussion

2.1. Melt-textured bulk materials

In Fig. 1a a FESEM image of a cleaved section of a YBCO melt-textured sample [9], irradiated on two opposite sides at a fluence of 1.21×10^{11} Au-ions/cm^2 (corresponding to a dose equivalent field $B_\varphi = 2.5$ T [10]), is shown. Sample thickness was chosen in such a way that the irradiated volume corresponds to about 10% of the whole sample thickness. Beside the presence of a lot of microscale intrinsic defects it is interesting to observe how, in this case, twin boundary defects nicely follow the column direction (see the magnification of Fig. 1c). Also a magnification of a column-treaded zone is shown in Fig. 1b.

* Corresponding author. Address: Dept. of Physics, Politecnico di Torino, C.so Duca degli Abruzzi 24, Torino 10129, Italy. Tel.: +39 011 564 7317; fax: +39 011 564 7399.
E-mail address: bruno.minetti@polito.it (B. Minetti).

0921-4534/$ - see front matter
doi:10.1016/j.physc.2010.02.057

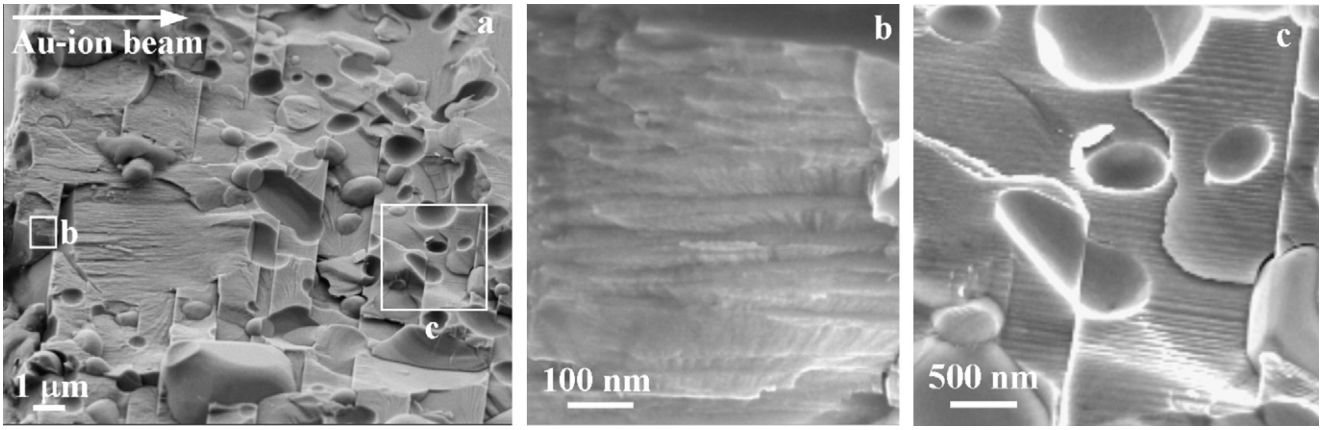

Fig. 1. (a) Melt-textured cross-section measured by FESEM (irradiated surface on left). Linearly correlated columnar defects are clearly visible at sample surface. (b) Magnification of a surface region crossed by columnar defects (see the corresponding frame in (a)). (c) Magnification of twin boundaries in a deeper region not reached by ion-induced columnar tracks (see the corresponding frame in (a)).

Due to the large variety (Fig. 1a) of candidate pinning centers, it is suitable to report the results of an "ad hoc" modified Dew-Hughes analysis [11,12] on pinning force (F_p) behavior as a function of magnetic field. The analysis allows selecting the contribution of main defect typologies (Fig. 2). In particular we fitted the experimental data with the formula $F_p(H) = \sum_i C_i H^{p_i}(H_{irr,i} - H)^{q_i}$ where C_i is a prefactor accounting for the defect relative contribution to the total F_p, $\mu_0 H_{irr,i}$ is the irreversibility field related to the considered defect typology, p_i and q_i are parameters depending on the intrinsic characteristics of the kind of defects whose value is predicted 'ex ante' by the Dew-Hughes model [11]. We considered both the prefactor and the irreversible field as fit parameters.

After acquiring F_p vs. $\mu_0 H$ curves before and after irradiation, this Dew-Hughes analysis separately evaluates the pinning force of the main single defect typologies as a function of the magnetic field and imposes the condition that their contribution sum must fit the experimental pre-irradiation and post-irradiation curves, respectively. From such analysis it turns out indeed that the calculated contribution of the columnar defects alone does not account for the huge experimental difference between the before and after irradiation curves. On the contrary the non-linear change of pinning force dependence on magnetic field for the various defect typologies (mainly Y-211 inclusions and twin boundary defects) firmly hints to a volume extended cooperative behavior between defects, supported by columns.

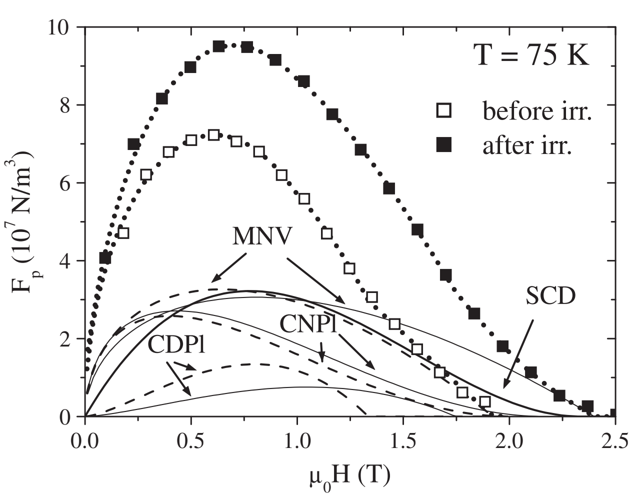

Fig. 2. Experimental pinning forces (symbols) as a function of the magnetic field before and after Au-ion irradiation at T = 75 K for a typical melt-textured sample. The contributions of the most effective pinning centers before (dashed lines) and after (solid lines) irradiation are reported. Legend: MNV = magnetic normal volume pinning centers (in our samples: Y-211 phase inclusions); CNPl = core normal planar pinning centers, as sub-grain boundaries or weakly-coupled grain boundaries (width higher than $2\xi_{ab}$); CDPl = core Δk planar pinning centers, i.e. nanosized extended defects as twin boundaries (width lower than $2\xi_{ab}$); SCD = surface columnar defects. The dotted lines represent the fits of the experimental data with the modified Dew-Hughes model.

2.2. Monofilamentary tapes

Ag/BSCCO-2223, 100 µm thick, monofilamentary tapes [13] were irradiated at a fluence of 0.48×10^{11} Au-ions/cm^2 (B_φ = 1 T). The Au-ion beam was directed perpendicularly to the tape surface. Also in this case the irradiated volume is about 10% of the whole useful volume.

The outstanding feature of FESEM imaging of these commercial BSCCO monofilamentary tapes, is the disordered tilting, up to large angles (about 40°) of different available space (Fig. 3). This structure then shows several voids, angle mismatches, etc. The FESEM picture clearly shows the columns crossing the surface sheet.

Among several volume experimental measurements such as critical current density evaluation and vortex confining modeling [14], it is worthwhile to emphasize in this case measurements of irreversibility temperature vs. external field applied at different angles with respect to the tape plane (Fig. 4). For our irradiation the dose equivalent field, B_φ was 1 T. The irreversibility line was considered in the range 0.02–5 T. We found the expected experimental

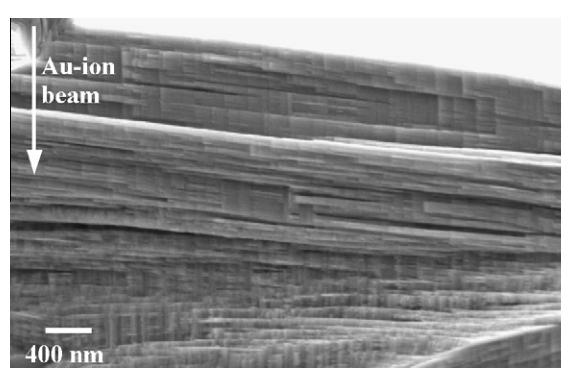

Fig. 3. Tape cross-section measured by FESEM (irradiated surface on top). Linearly correlated columnar defects induced by Au-ion irradiation are clearly visible.